Available online at www.sciencedirect.com
SCIENCE DIRECT
Thermochimica Acta 431 (2005) 62–67
thermochimica acta
www.elsevier.com/locate/tca

Thermal diffusivity of binary mixture of *n*-tricosane and *n*-tetracosane by Fourier transform temperature wave analysis

Naoko Miyamoto, Junko Morikawa, Toshimasa Hashimoto *

Graduate School of Science and Engineering, Tokyo Institute of Technology, 2-12-1, O-okayama, Meguro-ku, Tokyo 152-8552, Japan

Received 29 October 2004; received in revised form 10 January 2005; accepted 20 January 2005
Available online 23 February 2005

Abstract

The phase transitions of binary mixtures of *n*-tricosane ($C_{23}H_{48}$)/*n*-tetracosane ($C_{24}H_{50}$) are investigated by Fourier transform temperature wave analysis (FT-TWA) and differential scanning calorimetry (DSC). The phase diagram determined by both methods gives a good agreement. Thermal diffusivity shows an odd–even effect at the solid state, and the temperature dependence of thermal diffusivity of the mixture is classified into two types, odd-like type and even-like type, depending on the mixing ratio. The increase of thermal diffusivity in the rotator phase RI (orthorhombic rotator phase) prior to the phase transition to α-RII (rhombohedral rotator phase with hexagonal subcell) is found for odd number *n*-tricosane ($C_{23}H_{48}$). A detailed study of the rotator phase transition is shown by the measurement of thermal diffusivity.

Keywords: *n*-Alkanes; Rotater phase; *n*-Tricosane; *n*-Tetracosane; Odd–even effect; Fourier transform temperature wave analysis; Thermal diffusivity

1. Introduction

Polymorphic behavior of crystalline normal alkane (*n*-alkane) has been investigated in detail for a long time by various measuring techniques such as X-ray diffraction [1–3], differential scanning calorimetry (DSC), infrared (IR) and Raman spectroscopy [4], NMR [5], inelastic neutron scattering [6], and dielectric absorption [7]. A long-term vigorous study has clarified the basic science of linear hydrocarbons on the basis of the following view points:

(1) The crystallography of odd and even number *n*-alkanes, especially concerning the difference in the rotator phase. The even number *n*-alkanes give rise to rotator phase of type α-RII ($n \leq 26$; note, that a number of carbon atoms in a molecule is expressed as *n*) whereas odd-number *n*-alkanes ($n \leq 25$) give rise to rotator phase of type RI; where α-RII is rhombohedral rotator phase with hexagonal subcell with the space group *R*3*m*, and RI is orthorhombic rotator phase with the space group *Fmmm*.
(2) Solid–solid phase transitions prior to melting of hydrocarbon are considered as analogous pre-melting transitions found in more complex systems that contain hydrocarbon chains as major constituents. These systems include polyethylene, substituted alkanes, and biological membranes.

Broadhurst selected the published data, and classified the crystal system of *n*-alkanes (C_nH_{2n+2}) based on the even and the odd number of carbon atoms, *n* [8], and the precise crystallographic classification has been reported including the binary blend systems of *n*-alkanes [9–13] in the current study.

For instance, at room temperature, the crystal structure of odd-number *n*-alkane is orthorhombic, whereas even-number *n*-alkane with $n \leq 24$ is triclinic, or monoclinic with $n \geq 26$ [8]. The difference of crystal system between the odd and the even-number *n*-alkane originates in the difference of the ordered state of packing with the end methyl group. When the molecular chain axis is tilted in triclinic or monoclinic, only the molecular chain having the even number carbon atoms

* Corresponding author. Tel.: +81 357342435; fax: +81 357342435.
E-mail addresses: jmorikaw@o.cc.titech.ac.jp (J. Morikawa), toshimas@o.cc.titech.ac.jp (T. Hashimoto).

0040-6031/$ – see front matter © 2005 Elsevier B.V. All rights reserved.
doi:10.1016/j.tca.2005.01.040

can have the ordered symmetry state of end methyl group required for lower energy. If the odd number chain is tilted and one end group is assumed taking lower energy position, the other end group is forced to take a higher energy position. So, the odd number *n*-alkane is required to form no tilting structure like orthorhombic or hexagonal.

The crystal systems of the odd and the even number *n*-alkanes have been clarified with a variety of techniques. The lattice spacing and the lattice parameter have been precisely determined as a function of temperature by X-ray diffraction [4,14–17]. Heat capacity and relative specific entropy were studied by DSC [14,15]. However, the heat transport property, such as thermal conductivity or thermal diffusivity, of *n*-alkane has not yet been sufficiently studied. The authors reported thermal diffusivity of *n*-alkane and found a characteristic phenomenon related to the rotator phase, especially in crystal system of RI observed in *n*-tricosane (*n*-$C_{23}H_{48}$) [18] and *n*-pentacosane (*n*-$C_{25}H_{52}$) [19], also the specification of thermal diffusivity in the odd and the even number *n*-alkanes [20].

To clarify the relation with thermal diffusivity and the previously reported crystal systems, thermal diffusivity of the binary blend of *n*-tricosane (*n*-$C_{23}H_{48}$) and *n*-tetracosane (*n*-$C_{24}H_{50}$) are examined in this study, of which the phase diagram was previously determined by Sabour et al. and Dirand et al. based on the X-ray diffraction and DSC [10,11].

Temperature wave analysis (TWA) [18,21–23] and Fourier transform temperature wave analysis (FT-TWA) [19,20,24–27] have been developed for measuring thermal diffusivity of thin film. In particular FT-TWA enables simultaneous measurement of thermal diffusivity at multiple frequencies at a time in a temperature scan, therefore the frequency dependent thermal diffusivity is observed at a time, for example, in the glass transition of polymers [24–27] and the rotator phase transitions of *n*-pentacosane [19]. The frequency dependent thermal properties such as specific heat [28–31] and thermal effusivity [28,32] have also been studied by 3ω method, ac calorimetry and temperature modulated DSC.

In this study, the solid–solid phase transition prior to melting in the binary mixture of *n*-tricosane and *n*-tetracosane is investigated by the measurement of thermal diffusivity with the method of FT-TWA.

2. Experimental

2.1. Specimen

Two kinds of *n*-alkanes, *n*-tricosane (*n*-$C_{23}H_{48}$: hereafter abbreviated to C_{23}) and *n*-tetracosane (*n*-$C_{24}H_{50}$: C_{24}) were obtained from Tokyo Chemical Industry Co. Ltd. and were used without further purification. The purity grade was over 99 mol%.

The binary mixtures of various molar proportions, including pure-C23 and pure-C24, were prepared as listed in Table 1. Each mixture in the liquid state was sealed in the cell and pre-cooled at a rate of 0.5 °C/min to 25 °C. The sample for the measurement of DSC was prepared in the same procedure.

2.2. Measurements

The measurement of thermal diffusivity, α, was performed by using FT-TWA developed in our laboratory [24–27]. In this method, temperature wave is generated by ac Joule heating on the front surface of the film-shaped specimen, and then the temperature wave propagating in the specimen is detected on the rear surface. The square pulse train with a variable duty factor is used as the input of ac voltage. Detail of the computational procedure for solving the one-dimensional heat diffusion equation for temperature wave was described previously [24,27]; the phase delay of each *n*th order harmonic on the rear surface, $\Delta\theta_n$, is derived as follows:

$$\Delta\theta_n = -\sqrt{\frac{n\omega}{2\alpha}}d - \frac{\pi}{4} - an\pi \tag{1}$$

where ω is the angular frequency of the temperature wave, d the specimen thickness, a a duty factor of the input square pulse train, and n the order of harmonic. Eq. (1) is transformed into the following equation:

$$\alpha_n = \frac{n\omega}{2}\frac{d^2}{\left(\Delta\theta_n + \frac{\pi}{4} + an\pi\right)^2} \tag{2}$$

where thermal diffusivity is determined with the phase delay $\Delta\theta_n$ and the angular frequency $n\omega$ of each harmonic as a function of temperature.

Table 1
Experimental conditions and the characterized temperature of binary mixtures of *n*-tricosane and *n*-tetracosane

Samples		Temperature wave frequency (Hz)	Temperature (°C)					
C23:C24 (mol%)	Thickness (μm)		T_1	T_1'	T_1''	T_2	T_f	T_{em}
100:0	104	7–21	37.1	38.8	42.2	45.4	47.3	48.7
90:10	101	7–21	36.2	37.6	41.5	45.4	47.6	49.1
70:30	94	10–30	36.0	38.2	42.0	45.7	48.5	50.2
50:50	102	10–30	36.7	38.8	42.3	45.9	49.0	50.6
30:70	93	7–21	38.1	40.7	43.4	46.7	49.5	51.2
10:90	97	4–12	42.7	45.4	–	47.5	50.5	51.9
0:100	102	8–24	48.0	–	–	48.7	51.3	52.6

The thickness of the specimen was kept constant at a certain load with a spacer by setting the periphery of the specimen free in the cell. A duty factor a of the square pulse train input on the heater was set as 0.125. The frequency chosen for the measurement of each specimen was listed in Table 1. The amplitude of the temperature wave was selected to be less than 0.1 °C on the front surface. Phase delay at each harmonic, first to third, was measured as a function of temperature at a heating rate of 0.1 °C/min.

Perkin-Elmer DSC-7 was used for the measurement of heat capacity with 1–4 mg specimen of each mixture. The specimen was melted first and pre-cooled at a rate of 0.5 °C/min in an aluminum pan. The measurement was carried out at a heating rate of 0.5 °C/min in an atmosphere of nitrogen. The temperature calibration was carried out by indium and tin, and the heat flow rate was calibrated with the heat of fusion of indium.

3. Results and discussion

3.1. DSC measurement

Fig. 1 shows the heat capacity of the mixtures of C23 and C24. Each heat capacity curve shows two sharp and large endothermic peaks. Furthermore, the tiny endothermic peak is observed between these two peaks for six specimens except for pure-C24. As depicted in Fig. 1, each peak is named as s-1, s-2 and s-melting. The enthalpy ΔH of each transition in Fig. 1 is plotted against the molar concentration of C24 in Fig. 2. The melting enthalpy is regarded as almost constant irrespective of the C24 ratio. On the other hand, ΔH of s-1 changes depending on the ratio of C24, especially at the ratio more than 70 mol% of C24. The presence of another broad peak between s-1 and s-2 is also recognized in pure-C23, assumed corresponding to the peak reported by Dirand and coworkers [10,11] and Doucet et al. [14]. The peak position of this broad peak is named s-3p in the following.

3.2. Thermal diffusivity measurement

Fig. 3 shows thermal diffusivity of the C23 + C24 mixtures determined by first to third harmonics in the frequency range of 4–30 Hz at a heating rate of 0.1 °C/min. The thermal diffusivity of each mixture in the liquid phase at 55 °C is 0.81×10^{-7} m^2/s, so each result is plotted by a shift as depicted in Fig. 3. Pure-C23 and pure-C24 show the different temperature dependence of thermal diffusivity, which is considered as the so-called odd–even [33] effect for thermal diffusivity, the further is shown below.

Fig. 4 illustrates thermal diffusivity of (a) pure-C23 and (b) pure-C24, respectively, showing the definition of the characterized temperatures for each. For pure-C23, six of the characterized temperatures, T_1, T_1', T_1'', T_2, T_f and T_{em} are defined. On the other hand, four are defined, T_1, T_2, T_f and T_{em}, for pure-C24. T_f and T_{em} correspond to the temperatures at

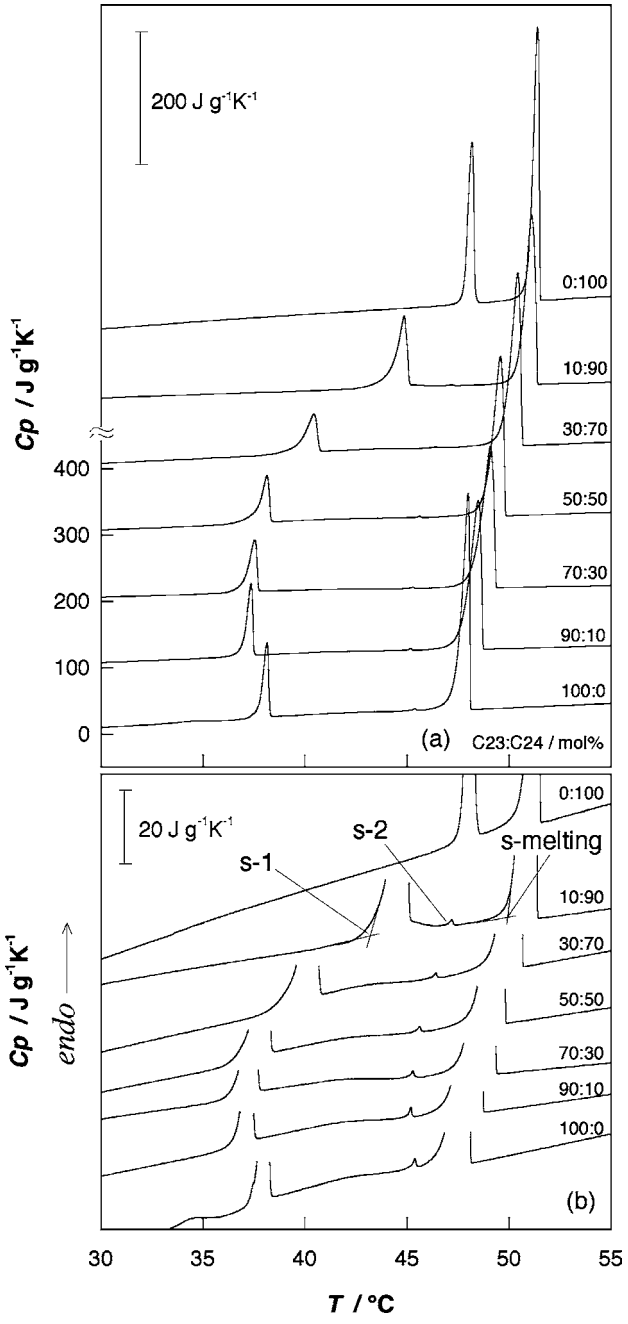

Fig. 1. Heat capacity of C23 + C24 mixtures with the heating rate of 0.5 °C/min: (a) normal drawing and (b) enlarged drawing.

which a partially melting starts and at which the specimen becomes isotropic liquid, respectively, by the observation with the polarized optical microscope. A significant difference of thermal diffusivity can be observed between pure-C23 and pure-C24, for example, T_1' (an initial temperature for the bottom plateau) and T_1'' (a completion temperature for the bottom plateau) are observed only for odd number C23, not for even number C24. The characterized temperatures of the mixtures are listed in Table 1, where T_1' and T_1'' are observed in the high C23 mol% range, 100–30 mol%, on the other hand, only T_1' is seen in 10 mol% of C23, and both are not observed in

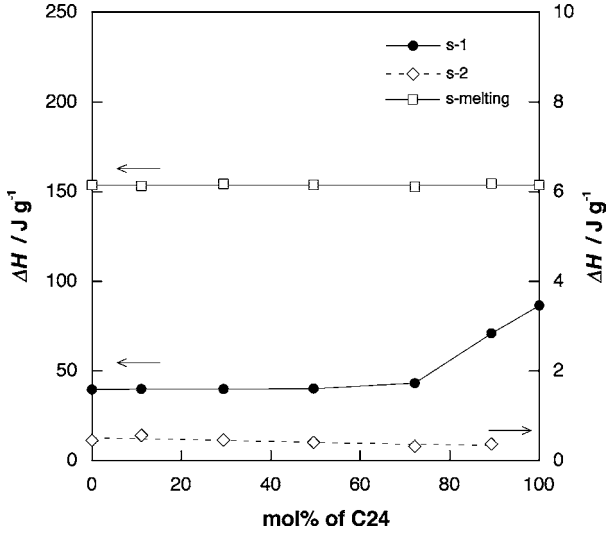

Fig. 2. Relationship between the transition enthalpy and the concentration of C24 for the C23 + C24 mixtures: (●) s-1; (◊) s-2; (□) s-melting.

pure-C24. Considering from a view point of the existence of T_1' and T_2'', the mixtures are classified into the odd-like type, and the even-like type, for example, those of 100–30 mol% of C23 are the odd-like type, 90 mol% of C24 is intermediate

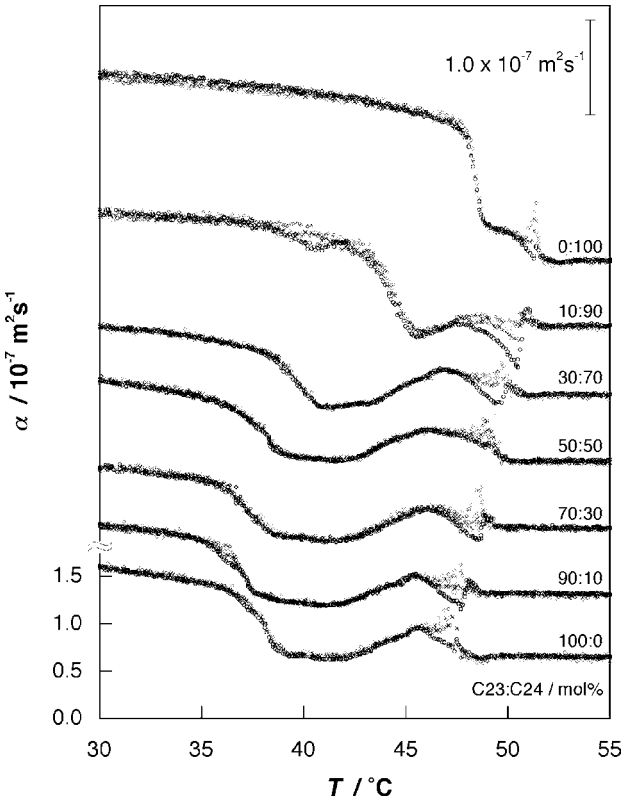

Fig. 3. Thermal diffusivity of C23 + C24 mixtures obtained from the phase delay of the first to the third harmonics in heating. The specimen thickness is about 100 μm. The heating rate is 0.1 °C/min, and a duty factor and the fundamental frequency of the temperature wave is 0.125 and 4–10 Hz. For each mixtures: (◯) first; (×) second; (◊) third harmonic.

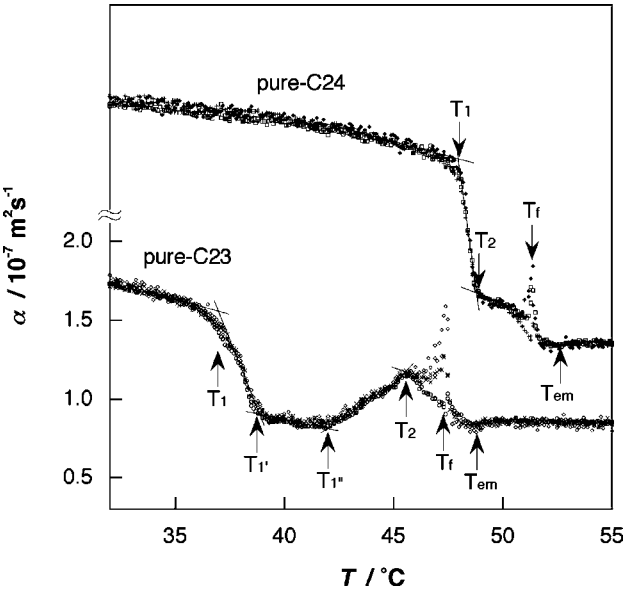

Fig. 4. Schematic diagram of the definition of the characterized temperature of thermal diffusivity.

between the odd and the even-like types, and pure-C24 is the even-like type.

The relationships between crystal systems previously determined by X-ray diffraction [4,10,11,14–17] and the transition temperatures (T_1, T_1', T_1'', T_2 and T_f) determined in this study by TWA are summarized as follows.

The characterized temperatures of $C_{23}H_{48}$ are attributed as:

- T_1: transition temperature from β_0' to β, corresponding to s-1 by DSC;
- T_2: transition temperature from RI to α-RII, corresponding to s-2 by DSC;
- T_f: transition temperature from α-RII to liquid state, corresponding to s-melting by DSC;
- T_1' and T_1'': not attributed [34].

The characteristic temperatures of $C_{24}H_{50}$ are attributed as:

- T_1 (T_2): transition temperature from γ to α-RII, corresponding to s-1 by DSC.
- T_f: transition temperature from α-RII to liquid state, corresponding to s-melting by DSC.

Notations and the schematic relationships between the crystal phases and the transition temperatures of $C_{23}H_{48}$ and $C_{24}H_{50}$ are shown in Table 2. The phase transition temperatures determined by TWA and DSC corresponds well also with the reported studies, although the attribution of T_1' and T_1'' is not clear at present [34].

The deviation from Eq. (1) observed in the rotator phase, between T_2 and T_f prior to melting, suggests the imaginary component of thermal diffusivity in this temperature range where the thermal diffusivity determined by Eq. (1) must be shown as the apparent value.

Table 2
Crystal phase and phase transition temperatures of $C_{23}H_{48}$ and $C_{24}H_{50}$

$C_{23}H_{48}$						
Crystal phase	β_0 →	β_0' →	β →	RI →	α-RII →	L
Transition temperature						
TWA	(T_δ)	T_1	T_1'	T_1''	T_2	T_f
DSC	(s_δ)	s-1		(s-3p)	s-2	s-melting
$C_{24}H_{50}$						
Crystal phase	γ →	α-RII →	L			
Transition temperature						
TWA	T_1 ~(T_2)	T_f				
DSC	s-1	s-melting				

Notations: crystal phases of $C_{23}H_{48}$ [11,12]; β_0: orthorhombic phase with the space group *Pbcm*; β_0': orthorhombic phase which appears above the transition δ; β: C-face centered rotator phase, or orthorhombic phase, or monoclinic phase with the space group *C*2/*c*; RI: orthorhombic rotator phase with the space group *Fmmm*; α-RII: rhombohedral rotator phase with hexagonal subcell, space group *R*3*m*; crystal phases of $C_{24}H_{50}$ [10,11]; γ: triclinic phase; α-RII: rhombohedral rotator phase with hexagonal subcell.

Fig. 5 shows thermal diffusivity of the C23 + C24 mixtures in the solids (25 °C) and in the liquids (55 °C). The thermal diffusivity of the mixture in the liquid state is independent on the mixing ratio. For *n*-alkanes and alkane derivatives, it has been reported that thermal diffusivity in the liquid state is independent on the number of carbon atoms, *n*, and the terminal functional group [24], where the molecular configuration is random and the molecular mobility is high. It is assumed that the heat transfer in the liquid phase will be performed between the adjacent molecules by the collision of the part of methylene unit, so thermal diffusivity is independent of the number of carbon atoms or the mixing ratio.

On the other hand, in the state of solid, thermal diffusivity depends on the mixing ratio. Thermal diffusivity of the C23 + C24 mixture is lower than that of pure-C23 or pure-C24. This result suggests the end methyl group effect on thermal diffusivity of the molecular crystal. That is, the presence of C24 causes the disorder of the crystallographic structure of C23, particularly of the regularity in the end methyl group plane, so that it can be assumed that the heat conduction will be scattered by the end-methyl group.

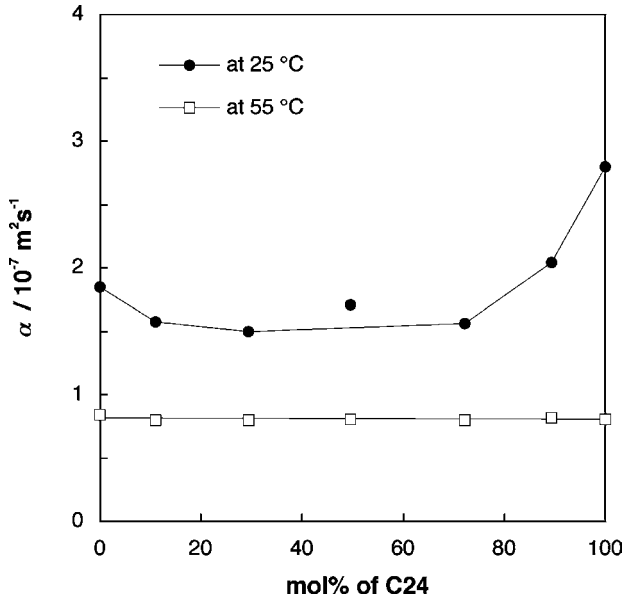

Fig. 5. Relationship between thermal diffusivity and the concentration of C24 for the C23 + C24 mixtures: (●) at the room temperature (25 °C); (□) in the liquid phase (55 °C).

3.3. Phase diagram

The phase diagram of the C23 + C24 mixtures is shown in Fig. 6. The solid curves in Fig. 6 are reported previously from Dirand and coworkers [10,11], the full symbols show the onset temperatures of the peaks (s-1, s-2, s-melting) observed by DSC in Fig. 1 and the empty symbols are the temperatures (T_1, T_1', T_1'', T_2 and T_f) defined in Fig. 4 by FT-TWA.

It is clarified that the characteristic temperatures (T_1, T_1', T_2, and T_f) of thermal diffusivity give a fairly good agreement with the phase transition temperatures determined by DSC and by Dirand et al. [11]. It means that the thermal diffusivity corresponds well to the identified crystal structure and the steep decrease or increase of thermal diffusivity corresponds to each phase transition as shown in Table 2. For instance, pure-C23 and mixtures up to 75 mol% of C24 undergo the transformation from orthorhombic to rotator phase (orthorhombic rotator phase (RI) to rhombohedral rotator phase (α-RII)), and finally to liquid phase with the temperature increase. On the other hand, pure-C24 shows the phase transition from triclinic to α-RII, and to liquid phase, and 90 mol% of C24 undergoes RI between triclinic and α-RII. The major

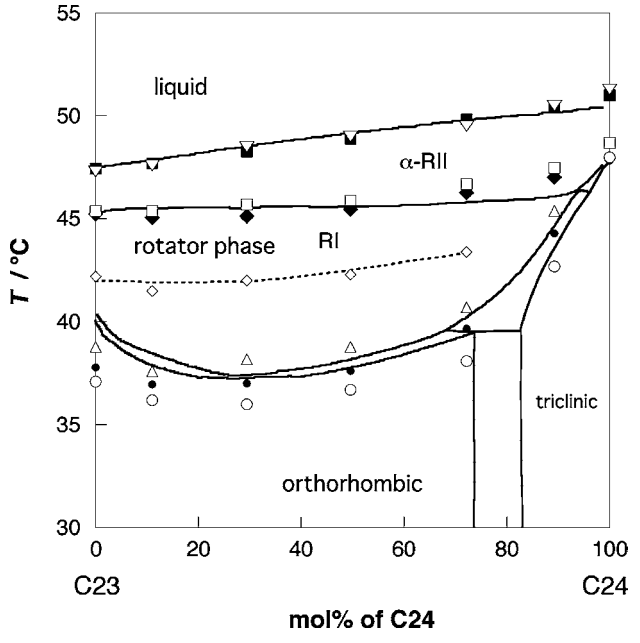

Fig. 6. Phase diagram of the C23 + C24 mixtures. The filled symbols ((●) s-1, (♦) s-2 and (■) s-melting) show the onset temperature of phase transition determined by DSC and the empty symbols ((◯) T_1, (△) T_1', (◇) T_1'', (□) T_2, (▽) T_f) are the characterized temperature of thermal diffusivity by FT-TWA. The solid curves are the previously reported phase diagram from Dirand et al. [12].

difference between each crystal system is the packing density in the plane of end methyl group and the tilt angle of the methylene chain to the end-methyl plane. Therefore, it is considered that the phonon mode at the interface of end-methyl plane dominates the thermal diffusion in the mixtures.

In view of the molar concentration (of C24) dependence of each characteristic temperature (T_f, T_2, T_1, T_1' and T_1''), it is understood that the odd–even effect disappears above T_2, where the total molecular weight of the mixture governs thermal diffusivity, and T_f or T_2 increases linearly with the molar concentration of C24. On the other hand, the mixed crystal structures of the odd and the even [11] below T_2 originate the complicated molar concentration (of C24) dependence of T_1, T_1' and T_1''.

In principle, temperature modulation technique takes an advantage less influenced by the latent heat. That is considered one reason for T_1' and T_1'' observed by FT-TWA.

4. Conclusions

The phase transitions of binary mixtures of *n*-tricosane ($C_{23}H_{48}$)/*n*-tetracosane ($C_{24}H_{50}$) were investigated by FT-TWA and DSC. The phase diagram determined by both methods gave a good agreement. Thermal diffusivity showed the odd-even effect at the solid state, and the temperature dependence of thermal diffusivity of the mixture was classified into the odd-like type and the even-like type depending on the mixing ratio. On the other hand, thermal diffusivity in the liquid state was independent on the mixing ratio.

The specific increase of thermal diffusivity in the rotator phase RI (at T_1'') prior to the phase transition into α-RII was clearly observed in odd number C23 and the mixtures of higher concentration of C23. Temperature modulation method for the measurement of thermal diffusivity is useful to study of the rotator phase transitions of molecular crystals.

References

[1] A. Müller, Proc. Roy. Soc. London A138 (1932) 514.
[2] A.A. Schaerer, C.J. Busso, A.E. Smith, L.B. Skinner, J. Am. Chem. Soc. 77 (1955) 2017.
[3] W. Piesczek, G.R. Strobl, K. Malzahn, Acta Cryst. B30 (1974) 1278.
[4] G. Ungar, N. Masic, J. Phys. Chem. 89 (1985) 1036.
[5] R.E. Dehl, J. Chem. Phys. 60 (1973) 339;
H.G. Olf, A. Peterlin, J. Polym. Sci., Part A-2 8 (1970) 791.
[6] D.H. Bonser, J.F. Barry, M.W. Newberry, M.V. Smalley, E. Granzer, C. Koberger, P.H. Nedwed, J. Sheidel, Chem. Phys. Lett. 62 (1979) 576.
[7] J.D. Hoffman, J. Chem. Phys. 20 (1952) 541.
[8] M.G. Broadhurst, J. Res. Natl. Bur. Std. 66A (1962) 241.
[9] A.R. Gerson, S.C. Nyburg, Acta Cryst. B50 (1994) 252.
[10] A. Sabour, J.B. Bourdet, M. Bouroukba, M. Dirand, Thermochim. Acta 249 (1995) 269.
[11] M. Dirand, Z. Achour, B. Jouti, A. Sabour, Mol. Cryst. Liq. Cryst. 275 (1996) 293.
[12] J. Fenrych, E.C. Reynhardt, I. Basson, Chem. Phys. Lett. 275 (1997) 215.
[13] I. Paunovic, A.K. Mehrotra, Thermochim. Acta 356 (2000) 27.
[14] J. Doucet, I. Denicolo, A. Craievich, A. Collet, J. Chem. Phys. 75 (1981) 5125.
[15] G. Ungar, J. Phys. Chem. 87 (1983) 689.
[16] A.F. Craievich, I. Denicolo, J. Doucet, Phys. Rev. B 30 (1984) 4782.
[17] I. Denicolo, J. Doucet, A.F. Craievich, J. Chem. Phys. 75 (1981) 1523.
[18] T. Tsuji, T. Hashimoto, Netsu Sokutei 19 (1992) 156.
[19] J. Morikawa, T. Hashimoto, Thermochim. Acta 352/353 (2000) 291.
[20] N. Miyamoto, J. Morikawa, T. Hashimoto, Netsu Sokutei 30 (2003) 98.
[21] T. Hashimoto, Y. Matsui, A. Hagiwara, A. Miyamoto, Thermochim. Acta 163 (1990) 317.
[22] T. Kurihara, J. Morikawa, T. Hashimoto, Int. J. Thermophys. 18 (1997) 505.
[23] T. Hashimoto, J. Morikawa, T. Kurihara, T. Tsuji, Thermochim. Acta 304/305 (1997) 151.
[24] J. Morikawa, T. Hashimoto, Jpn. J. Appl. Phys. 37 (1998) 1484.
[25] T. Hashimoto, J. Morikawa, Netsu Sokutei 27 (2000) 141.
[26] J. Morikawa, T. Hashimoto, J. Therm. Anal. Cal. 64 (2001) 403.
[27] J. Morikawa, T. Hashimoto, A. Maesono, High Temp. High Press. 133 (2001) 387.
[28] A.A. Minakov, S.A. Adamovsky, C. Schick, Thermochim. Acta 403 (2003) 89.
[29] M. Reading, A. Luget, R. Wilson, Thermochim. Acta 238 (1994) 295.
[30] B. Wunderlich, Y. Jin, A. Boller, Thermochim. Acta 238 (1994) 277.
[31] J.E.K. Schawe, Thermochim. Acta 260 (1995) 1;
J.E.K. Schawe, Thermochim. Acta 261 (1995) 183;
J.E.K. Schawe, Thermochim. Acta 271 (1996) 127.
[32] N.O. Birge, S.R. Nagel, Phys. Rev. Lett. 54 (1985) 2674.
[33] W.R. Turner, Ind. Eng. Chem. Prod. Res. Dev. 10 (1971) 238.
[34] The relationship between (i) T_1'' and s-3p (by DSC in this study) and (ii) the relation with the temperature for lattice parameter change in Ref. [30] are suggested.